

1 **Fungal derived 15-keto-prostaglandin E<sub>2</sub> and host proliferator-activated receptor gamma (PPAR- $\gamma$ )**  
2 **promote *C. neoformans* growth during infection.**

3 **Authors:**

4 **Robert J. Evans<sup>1,2</sup>, Sarah Needs<sup>3</sup>, Ewa Bielska<sup>3</sup>, Robin C. May<sup>3,4</sup>, Stephen A. Renshaw<sup>1,2</sup>, Simon A.**  
5 **Johnston<sup>1,2</sup>**

6 <sup>1</sup> Bateson Centre, Firth Court, University of Sheffield, S10 2TN, UK.

7 <sup>2</sup> Department of Infection, Immunity and Cardiovascular Disease, Medical School, University of Sheffield,  
8 S10 2RX, UK.

9 <sup>3</sup> Institute of Microbiology and Infection, School of Biosciences, University of Birmingham, Birmingham, B15  
10 2TT, UK.

11 <sup>4</sup> NIHR Surgical Reconstruction and Microbiology Research Centre, University Hospitals of Birmingham  
12 NHS Foundation Trust, Queen Elizabeth Hospital, Birmingham, UK

13

14 Running Title: Fungal derived 15-keto-prostaglandin E<sub>2</sub> and PPAR- $\gamma$  promotes *C. neoformans* infection

15

16

17

18

19

20

21 \*Author for correspondence: Simon A. Johnston

22 Email: s.a.johnston@sheffield.ac.uk

23 Phone: +44 114 222 2301

24 **Abstract**

25 *Cryptococcus neoformans* is one of the leading causes of invasive fungal infection in humans worldwide.  
26 *C. neoformans* can use macrophages as a proliferative niche to increase infective burden and avoid  
27 immune surveillance. However, the specific mechanisms by which *C. neoformans* manipulates host  
28 immunity to promote its growth during infection remain ill-defined. Here we demonstrate a key role for  
29 eicosanoid lipid mediators produced by *C. neoformans* in regulating host responses. *C. neoformans* is  
30 known to secrete several eicosanoids that are highly similar to those found in vertebrate hosts. Using the  
31 eicosanoid deficient cryptococcal mutant  $\Delta plb1$ , we demonstrate that prostaglandin E<sub>2</sub> is required by *C.*  
32 *neoformans* for proliferation within macrophages and, using our zebrafish model of cryptococcosis, we  
33 confirm this role for PGE<sub>2</sub> *in vivo*. Furthermore, we show that PGE<sub>2</sub> must be dehydrogenated into 15-keto  
34 PGE<sub>2</sub> to promote fungal growth. We find that activation of the intracellular 15-keto PGE<sub>2</sub> receptor PPAR- $\gamma$   
35 promotes fungal burden in zebrafish suggesting that cryptococcal 15-keto-PGE<sub>2</sub> is a novel virulence factor  
36 that may act as an agonist for PPAR- $\gamma$ .

37

38

39 **Author Summary:**

40 *Cryptococcus neoformans* is an opportunistic fungal pathogen that is responsible for significant  
41 numbers of deaths in the immunocompromised population worldwide. Here we address whether  
42 eicosanoids produced by *C. neoformans* manipulate host innate immune cells during infection.  
43 *Cryptococcus neoformans* produces a number of eicosanoids that are notable for their similarity  
44 to vertebrate eicosanoids, it is therefore possible that fungal-derived eicosanoids may mimic  
45 physiological effects in the host. Using a combination of *in vitro* and *in vivo* infection models we  
46 identify a specific eicosanoid species - prostaglandin E<sub>2</sub> – that is required by *C. neoformans* for  
47 growth during infection. We subsequently find that prostaglandin E<sub>2</sub> must be converted to 15-keto  
48 prostaglandin E<sub>2</sub> within the host before it has these effects. Furthermore, we provide evidence  
49 that the mechanism of prostaglandin E<sub>2</sub>/15-keto prostaglandin E<sub>2</sub> mediated virulence is via  
50 activation of host PPAR- $\gamma$  – an intracellular eicosanoid receptor known to interact with 15-keto PGE<sub>2</sub>.

## 51 Introduction

52 *Cryptococcus neoformans* is an opportunistic pathogen and that infects individuals who have severe  
53 immunodeficiencies such as late-stage HIV infection. *C. neoformans* is estimated to infect up to 1 million  
54 individuals each year globally and causes hundreds of thousands of deaths (1,2). *C. neoformans* infection  
55 begins as a respiratory infection but in the absence of an effective immune response the fungus  
56 disseminates to the central nervous system causing meningitis, and eventually death (3,4). *C. neoformans*  
57 initially grows within the alveolar spaces of the lungs as budding yeast before it is phagocytosed by  
58 macrophages. In normal immunity, macrophages must become activated by further inflammatory signals  
59 from the host immune system before they can effectively kill *C. neoformans* (5,6). When this does not occur  
60 macrophages cannot kill *C. neoformans*; instead the fungus is able to proliferate rapidly intracellularly and  
61 may use macrophages to disseminate to the central nervous system where it causes fatal meningitis (7-9).

62  
63 An important group of inflammatory mediators produced during the initial stages of microbial infection by  
64 macrophages are eicosanoids. Eicosanoids are a diverse group of potent lipid signalling molecules that  
65 have a short range of action and communicate through autocrine or paracrine routes. During infection  
66 macrophages produce large amounts of a particular group of eicosanoids called prostaglandins (10,11).  
67 Prostaglandins have a number of physiological effects throughout the body, but in the context of immunity  
68 they are known to strongly influence the inflammatory state(12). Two particular prostaglandins - PGE<sub>2</sub> and  
69 PGD<sub>2</sub> – are the best-studied eicosanoid inflammatory mediators. During infection macrophages produce  
70 both PGE<sub>2</sub> and PGD<sub>2</sub> and, via autocrine routes, macrophages are highly responsive to PGE<sub>2</sub> and PGD<sub>2</sub>  
71 (12). In vertebrate immunity, the synthesis of eicosanoids such as PGE<sub>2</sub> is carefully regulated by feedback  
72 loops to ensure that the potent effects of these molecules are properly constrained. Exogenous sources of  
73 eicosanoids within the body, such as from eicosanoid-producing parasites (13) or tumours that overproduce  
74 eicosanoids (14,15), disrupt host inflammatory signaling as they are not subject to the same regulation.

75  
76 During infection, *C. neoformans* produces a range of eicosanoid species which are indistinguishable from  
77 those produced by their vertebrate hosts (16-18). Currently only two *C. neoformans* enzymes -  
78 phospholipase B1 and laccase - are known to be associated with cryptococcal eicosanoid synthesis (18,19).

79 Deletion of phospholipase B1 reduces secreted levels of all eicosanoids produced by *C. neoformans*  
80 suggesting that it has high level role in eicosanoid synthesis (19), perhaps fulfilling the role of phospholipase  
81 A<sub>2</sub> in higher organisms. In contrast, it is possible that the cryptococcal enzyme has putative PGE<sub>2</sub> synthase  
82 activity (18). The synthesis of eicosanoids by *C. neoformans* raises the possibility that the fungus is able to  
83 manipulate host inflammation by directly manipulating host eicosanoid signaling during establishment of  
84 infection *in vivo*. During respiratory infection of mice, the inhibition of prostaglandin E<sub>2</sub> receptors EP2 and  
85 EP4 leads to better host survival accompanied by a shift towards Th1/M1 macrophage activation (20).  
86 Therefore, a key aspect of *C. neoformans* pathogenesis remains unanswered; do eicosanoids produced by  
87 *C. neoformans* manipulate host innate immune cells function during infection?

88  
89 We hypothesised that eicosanoids produced by *C. neoformans* were able to promote intracellular  
90 proliferation within macrophages and virulence in the host. We have previously shown that the  
91 phospholipase B1 deficient strain  $\Delta plb1$ , that lacks eicosanoid synthesis, cannot replicate or survive within  
92 macrophages (21). Thus, we sought to determine whether this deficiency is directly due to lower levels of  
93 eicosanoids produced by *C. neoformans*. To address this question we have combined *in vitro* macrophage  
94 infection assays with our previous published *in vivo* zebrafish model of cryptococcosis (22). Using this  
95 approach, we show that prostaglandin E<sub>2</sub> is sufficient to promote growth of the  $\Delta plb1$  during *in vitro* infection  
96 of macrophages. We find that this eicosanoid is also able to promote growth of *C. neoformans in vivo* but  
97 activity requires the dehydrogenation of PGE<sub>2</sub> into 15-keto PGE<sub>2</sub>, and the activity of the 15-keto PGE<sub>2</sub>  
98 receptor PPAR- $\gamma$ .

99

100

101

102

103

104

## 105 **Results**

### 106 *C. neoformans* prostaglandin $E_2$ is required for growth in macrophages

107 We have shown previously that the *C. neoformans* *PLB1* gene (coding for the secreted enzyme  
108 phospholipase B1) deletion mutant  $\Delta plb1$  (23) has impaired proliferation and survival during infection of  
109 J774 murine macrophages *in vitro* (21). It has been proposed that the attenuation of  $\Delta plb1$  could be because  
110 this strain cannot produce eicosanoids such as  $PGE_2$  which could be used by *C. neoformans* to interfere  
111 with macrophage activation (19).

112

113 To establish if *C. neoformans* requires  $PGE_2$  synthesis for growth within macrophages we investigated  
114 whether the intracellular proliferation defect of  $\Delta plb1$  could be rescued with the addition of exogenous  $PGE_2$   
115 to infected cells. We found that the addition of exogenous  $PGE_2$  to  $\Delta plb1$  infected J774 macrophages was  
116 sufficient to partially recover the intracellular proliferation rate (IPR) of  $\Delta plb1$  compared to its parental strain  
117 H99 (Fig 1A). These findings support our hypothesis that eicosanoid synthesis by *C. neoformans* is required  
118 to promote proliferation of the fungus during macrophage infection, furthermore they identify  $PGE_2$  as a  
119 mediator of cryptococcal virulence during macrophage infection.

120

### 121 *Phospholipase B1 dependent secreted factors are produced by C. neoformans to promote macrophage* 122 *infection*

123

124 After finding that  $PGE_2$  is required by *C. neoformans* to proliferate within macrophages, we next wanted to  
125 determine whether *C. neoformans* is the source of this growth promoting factor during macrophage  
126 infection. To test if *C. neoformans* produces phospholipase B1 dependent secretory factors, such as  $PGE_2$ ,  
127 to promote intracellular growth we used a co-infection assay which has previously been used to investigate  
128 the interaction of different *C. gattii* strains within the same macrophage (24). If the parental strain H99  
129 produces growth promoting factors that  $\Delta plb1$  cannot, we reasoned that  $\Delta plb1$  cells would display improved  
130 intracellular replication when H99 was also present within the same macrophage.

131

132 To produce co-infection, we infected macrophages with a 50:50 mixture of  $\Delta plb1$  and H99-GFP (25) (Fig  
133 2B i; as described previously for *C. gattii* (24)). The intracellular proliferation of  $\Delta plb1$  was calculated by  
134 counting the change in number of non-fluorescent  $\Delta plb1$  cells over an 18hr period from time-lapse movies  
135 of infected cells. Although we infected our macrophages with a 50:50 mixture of  $\Delta plb1$  and H99-GFP we  
136 found that co-infected macrophages did not always contain the same ratio of each strain. To control for  
137 differences in burden between macrophages, we only scored macrophages that had an initial burden of  
138 two  $\Delta plb1$  yeast cells to one H99-GFP yeast cell or vice versa. Interestingly we found that  $\Delta plb1$  (Fig 1B)  
139 proliferated better when accompanied by two H99-GFP yeast cells in the same macrophage (Fig 1 B ii, 1:2)  
140 as opposed to when two  $\Delta plb1$  yeast cells were accompanied by one H99-GFP yeast cell (Fig 1 B ii, 2:1).  
141 This suggests that there is a secreted factor produced by H99, but absent in  $\Delta plb1$  that can promote  
142 intracellular proliferation within macrophages.

143

144 *PGE<sub>2</sub> synthesis by C. neoformans is required for growth in vivo.*

145

146 After showing that PGE<sub>2</sub> produced by *C. neoformans* promotes *in vitro* fungal growth within macrophages  
147 we wanted to see if these interactions could be reproduced *in vivo*. Zebrafish have been proven to be an  
148 excellent model for understanding vertebrate eicosanoid biology (26,27) so we chose to investigate these  
149 interactions using our zebrafish model of cryptococcosis (22). One of the advantages of this infection model  
150 is that because we use fluorescently tagged *C. neoformans* strains, the fungal burden within infected larvae  
151 can be non-invasively imaged throughout infection. To use  $\Delta plb1$  with our zebrafish larvae infection model  
152 we generated a constitutively expressed GFP tagged version of the  $\Delta plb1$  ( $\Delta plb1$ -GFP). We next evaluated  
153 the growth of  $\Delta plb1$ -GFP by infecting zebrafish larval with  $\Delta plb1$ -GFP and measuring the growth of the  
154 fungus at 1,2 and 3 days post infection (dpi). Analysis of fungal burden revealed that  $\Delta plb1$ -GFP had a  
155 lower fungal burden at 1, 2 and 3 days post infection compared to the parental strain H99-GFP (Fig 2A, C).  
156 These data show that the  $\Delta plb1$  mutant has a similar growth deficiency in our *in vivo* model to our *in vitro*  
157 data and previous studies (21,23,28).

158

159 After confirming that fungal burden is reduced *in vivo*, we next wanted to investigate if this phenotype was  
160 due to an inability to generate PGE<sub>2</sub>. We treated  $\Delta plb1$  and H99 infections with PGE<sub>2</sub> and PGD<sub>2</sub> (PGD<sub>2</sub>  
161 tends to produce context-dependent opposing immune signalling to PGE<sub>2</sub> (15)). PGE<sub>2</sub>, but not PGD<sub>2</sub>,  
162 increased fungal burden of both the parental H99 strain (Fig 2B,  $p = 0.0137$ , 1.35-fold increase vs. DMSO)  
163 and the  $\Delta plb1$ -GFP mutant (Fig 2F,  $p = 0.0001$ , 2.15-fold increase vs. DMSO). Taken together these data  
164 show that PGE<sub>2</sub> is required for growth *in vivo*; this is in agreement with our *in vitro* findings suggesting that  
165 growth *in vivo* may rely on eicosanoid production during macrophage infection.

166

167 *Prostaglandin E<sub>2</sub> must be dehydrogenated into 15-keto-PGE<sub>2</sub> in order to facilitate C. neoformans growth.*

168

169 PGE<sub>2</sub> produced by *C. neoformans* can be further converted into 15-keto-PGE<sub>2</sub> (18). Due to the possibility  
170 that some of the PGE<sub>2</sub> added to zebrafish might be converted to 15-keto-PGE<sub>2</sub> we wanted to determine if  
171 the effects we observed were due to the activity of PGE<sub>2</sub> or 15-keto-PGE<sub>2</sub>. To test this, we treated infected  
172 larvae with 16,16-dimethyl PGE<sub>2</sub>, which cannot be dehydrogenated into 15-keto-PGE<sub>2</sub>, but otherwise has  
173 comparable activity to PGE<sub>2</sub> (29). Interestingly, in contrast to PGE<sub>2</sub>, we found that 16,16-dimethyl PGE<sub>2</sub>  
174 treatment did not increase the fungal burden of  $\Delta plb1$ -GFP (Fig 4E and 4G,  $p = 0.9782$ ) or H99-GFP infected  
175 larvae (Fig 4A and 4C,  $p = 0.9954$ ). To confirm that *C. neoformans* growth rate is facilitated by 15-keto-  
176 PGE<sub>2</sub> we treated infected larvae with exogenous 15-keto-PGE<sub>2</sub> and found that this was sufficient to  
177 significantly increase the fungal burden of both  $\Delta plb1$ -GFP (Fig 4F and 4H,  $p = 0.0119$ , 1.56-fold increase  
178 vs. DMSO) and H99-GFP infections (Fig 4B and 4C,  $p = 0.0048$ , 1.36-fold increase vs. DMSO). Taken  
179 together, these results demonstrated that the increase in *C. neoformans* burden we observed with PGE<sub>2</sub>  
180 treatment for both  $\Delta plb1$ -GFP and H99-GFP were due to dehydrogenation of PGE<sub>2</sub> into 15-keto-PGE<sub>2</sub>.

181

182

183 *15-keto-PGE<sub>2</sub> promotes C. neoformans growth by activating host PPAR- $\gamma$*

184

185 We next wanted to determine if 15-keto-PGE<sub>2</sub> is able to promote cryptococcal growth by interfering with  
186 host eicosanoid signalling pathways. 16,16-dimethyl PGE<sub>2</sub> signals through the same host receptors as

187 PGE<sub>2</sub> so its lack of activity in this system strongly suggests different molecular pathways for 15-keto PGE<sub>2</sub>  
188 and PGE<sub>2</sub>. With 15-keto PGE<sub>2</sub> has been reported as an agonist at the peroxisome proliferation associated  
189 receptor gamma (PPAR- $\gamma$ ) (30); a transcription factor that controls expression of many inflammation  
190 related. To determine if 15-keto PGE<sub>2</sub> promotes the growth of *C. neoformans* during host infection by  
191 activating host PPAR- $\gamma$  we treated infected larvae with a specific agonist of PPAR- $\gamma$  - Troglitazone (TLT) -  
192 at a concentration (0.55  $\mu$ M) shown to strongly activate PPAR- $\gamma$  in zebrafish larvae (31). We found that TLT  
193 treatment produced a significantly increased the fungal burden of  $\Delta plb1$ -GFP (Fig 5B and 5D,  $p = 0.0089$ ,  
194 1.68-fold increase vs. DMSO) and H99-GFP (Fig 5A and 5C,  $p = 0.0044$ , 1.46-fold increase vs. DMSO)  
195 infected larvae similar to 15-keto PGE<sub>2</sub> treatment. These findings suggest that 15-keto PGE<sub>2</sub> promotes  
196 fungal growth by activating PPAR- $\gamma$ .

197  
198 In conclusion, we have shown for the first time that eicosanoids produced by *C. neoformans* are required  
199 for virulence both *in vitro* and *in vivo*. We have shown that the intracellular growth defect of  $\Delta plb1$  (21,23)  
200 can be rescued with the addition of exogenous PGE<sub>2</sub> (Fig 1A). Furthermore, with our co-infection  
201 experiments we provide evidence that the source of this eicosanoid during infection is from the pathogen,  
202 rather than the host (Fig 1 B). Using a zebrafish larvae *in vivo* model of cryptococcosis we have gone on to  
203 show that a recently described fungal burden defect during larval infection can also be rescued with the  
204 addition of PGE<sub>2</sub> (Fig 2). Additionally we find that that PGE<sub>2</sub> appears to require dehydrogenated into 15-  
205 keto PGE<sub>2</sub> before it has a biological effect (Fig 2 and 3). Finally, we provide evidence that the mechanism  
206 of PGE<sub>2</sub>/15-keto PGE<sub>2</sub> mediated growth promotion during larval infection may be via the activation of  
207 PPAR- $\gamma$  – an intracellular receptor within macrophages that 15-keto PGE<sub>2</sub> is thought to activate.

208

209

210

211

## 212 Discussion

213 We have identified an unknown mechanism used by *C. neoformans* to manipulate host innate immunity  
214 whereby eicosanoids secreted by the fungus are able to manipulate the function of macrophages and  
215 promote fungal growth in the host through 15-keto PGE<sub>2</sub> and the host receptor PPAR- $\gamma$ .

216 We have previously identified that the *PLB1* gene deletion mutant  $\Delta plb1$  was deficient in replication and  
217 survival in macrophages (21), an observation also supported by a number of studies using different *in vitro*  
218 infection assays (19,23). In this study we have shown that the treating  $\Delta plb1$  infected macrophages with  
219 exogenous prostaglandin E<sub>2</sub> is sufficient to restore intracellular proliferation of  $\Delta plb1$ . During cryptococcal  
220 respiratory infection it has been observed that PGE<sub>2</sub> levels increase significantly in the lung (20). Our study  
221 identifies cryptococci as the source of PGE<sub>2</sub> and additionally it identifies the direct effect of PGE<sub>2</sub> on  
222 *Cryptococcus* intracellular proliferation, confirming PGE<sub>2</sub> as virulence factor required for growth in  
223 macrophages. As a PGE<sub>2</sub> is a phospholipase B1 dependent factor we hypothesised that co-infection would  
224 also be sufficient to recover intracellular growth in macrophages. Analysis of complementary ratios of  
225 mutant to parental strain numbers in co-infected macrophages demonstrated rescue, supporting our  
226 conclusion that cryptococcal derived PGE<sub>2</sub> is required for virulence.

227 A key goal of this study was to investigate how eicosanoids produced by *C. neoformans* may affect  
228 pathogenesis within a living host. We chose to use a zebrafish larvae model of cryptococcosis that our  
229 group has recently developed (22). To facilitate non-invasive fungal burden measurement within live larvae  
230 we created a GFP-tagged  $\Delta plb1$  strain with constitutive expression ( $\Delta plb1$ -GFP) to use alongside the GFP-  
231 tagged H99 parental strain we have previously produced (25). To our knowledge this is the first GFP tagged  
232 version of  $\Delta plb1$  created, and it also represents one of the only examples of a fluorescently tagged mutant  
233 *C. neoformans* strain. Characterisation of  $\Delta plb1$ -GFP using our zebrafish model of cryptococcosis revealed  
234 that this strain also has significantly reduced growth *in vivo* compared to H99-GFP, these findings confirm  
235 findings from a similar zebrafish cryptococcosis model which also found that  $\Delta plb1$  (non-fluorescent) had  
236 attenuated burden during larval infection (32).

237 To ascertain whether PGE<sub>2</sub> is also required for cryptococcal growth *in vivo* we treated zebrafish larvae  
238 infected with  $\Delta plb1$ -GFP or H99-GFP with exogenous PGE<sub>2</sub>. In agreement with our *in vitro* findings we

239 found that PGE<sub>2</sub> significantly improved the growth of *Δplb1-GFP* within larvae. Interestingly we also found  
240 that PGE<sub>2</sub> improved the growth of our H99-GFP parental control perhaps representing a wider manipulation  
241 of host immunity in *in vivo* infection. During larval infection, *C. neoformans* interacts closely with  
242 macrophages, it is therefore likely that the PGE<sub>2</sub> dependent growth observed in our *in vivo* model is due to  
243 host macrophage manipulation facilitated by *Cryptococcus* derived eicosanoids.

244 In vertebrate cells, PGE<sub>2</sub> is converted into 15-keto PGE<sub>2</sub> by the dehydrogenase enzyme 15-prostaglandin  
245 dehydrogenase (15PGDH). To determine whether the biological effect we observed with PGE<sub>2</sub> were  
246 affected by the conversion of to PGE<sub>2</sub> or 15-keto PGE<sub>2</sub> we treated infected larvae with 16,16 dm-PGE<sub>2</sub> – a  
247 synthetic variant of PGE<sub>2</sub> which is resistant to dehydrogenation (29). Interestingly we found that 16,16 dm-  
248 PGE<sub>2</sub> was not able to promote the growth of *Δplb1-GFP* or H99-GFP within infected larvae. These findings  
249 indicated that 15-keto PGE<sub>2</sub>, rather than PGE<sub>2</sub>, was the bioactive molecule during cryptococcal infection.  
250 To confirm these findings, we treated infected larvae with exogenous 15-keto-PGE<sub>2</sub> and found that 15-keto-  
251 PGE<sub>2</sub> treatment was sufficient to promote the growth of both *Δplb1-GFP* and H99-GFP without the need for  
252 PGE<sub>2</sub>. We propose that PGE<sub>2</sub> produced by *C. neoformans* is enzymatically dehydrogenated into 15-keto  
253 PGE<sub>2</sub>, as previously mentioned the vertebrate enzyme 15PGDH can convert PGE<sub>2</sub> into 15-keto PGE<sub>2</sub>,  
254 additionally it has been reported that *C. neoformans* itself has enzymatic activity analogous to 15PGDH  
255 (18), therefore it is possible that *C. neoformans* may produce both PGE<sub>2</sub> and 15-keto-PGE<sub>2</sub>. These findings  
256 represent the identification of a new virulence factor produced by *C. neoformans* as well as the first time  
257 that an eicosanoid other than PGE<sub>2</sub> has been identified as promoting cryptococcal growth. Furthermore,  
258 our findings suggest that previous studies which identify PGE<sub>2</sub> as a promoter of cryptococcal virulence  
259 (19,20,33) may have observed multiplicative effects from both PGE<sub>2</sub> and 15-keto PGE<sub>2</sub> activity.

260

261 The biological activity of 15-keto PGE<sub>2</sub> is far less studied than its parent species PGE<sub>2</sub>. 15-keto PGE<sub>2</sub> is  
262 unable to bind to the prostaglandin E<sub>2</sub> EP receptors which means that one of its physiological functions is  
263 to act as a negative regulator of PGE<sub>2</sub> activity i.e. cells up-regulate 15PGDH activity to lower PGE<sub>2</sub> levels  
264 (34). As our findings showed that 15-keto PGE<sub>2</sub> does have an effect during *C. neoformans* infection, we  
265 next sought the cellular receptor for 15-keto PGE<sub>2</sub>. With this in mind it has been demonstrated that 15-keto

266 PGE<sub>2</sub> is an agonist for the intracellular eicosanoid receptor peroxisome proliferator associated receptor  
267 gamma (PPAR-  $\gamma$ ) (30). PPAR-  $\gamma$  is a nuclear receptor normally found within the cytosol, upon ligand  
268 binding PPAR-  $\gamma$  forms a heterodimer with Retinoid X receptor (RXR) and translocates to the nucleus where  
269 it influences the expression of target genes which possess a peroxisome proliferation hormone response  
270 element (PPRE) (35).

271 Activation of PPAR-  $\gamma$  by *C. neoformans* has not been described previously but agrees with what we know  
272 of cryptococcal pathogenesis. PPAR-  $\gamma$  is an intracellular receptor found in many cell types including  
273 macrophages, if eicosanoids are being produced by *C. neoformans* during intracellular infection it is also  
274 likelier that they have bind to an eicosanoid receptor within the macrophage. Finally, activation of PPAR-  $\gamma$   
275 promotes the expression of genes that are anti-inflammatory, and in macrophages PPAR-  $\gamma$  activation can  
276 lead to alternative activation. The growth promoting effects of 15-keto PGE<sub>2</sub> and the identification of PPAR-  
277  $\gamma$  as a receptor for PPAR-  $\gamma$  led us to hypothesise that the effect of 15-keto PGE<sub>2</sub> could be mediated by  
278 PPAR-  $\gamma$  mediated activation of anti-inflammatory target genes. To establish whether PPAR-  $\gamma$  activation  
279 could promote the growth of *C. neoformans* in our zebrafish model we treated infected larvae with the drug  
280 troglitazone - a specific PPAR-  $\gamma$  agonist – at a concentration previously shown to activate PPAR-  $\gamma$  in  
281 zebrafish larvae. At this concentration we found that troglitazone was able to increase the growth of  $\Delta plb1$ -  
282 GFP and H99-GFP during infection. Although these findings strongly suggest that the cryptococcal growth  
283 promoting effects of 15-keto PGE<sub>2</sub> may mediated via activation of PPAR-  $\gamma$ , further work will be needed to  
284 prove that the effects we observe when PPAR-  $\gamma$  is activated by troglitazone are due to the activity 15-keto  
285 PGE<sub>2</sub>.

286 In conclusion we have shown for the first time that synthesis of eicosanoids by *C. neoformans* is able to  
287 promote intracellular growth within macrophages and within an *in vivo* host. Additionally, we have  
288 uncovered a new virulence factor – 15-keto-PGE<sub>2</sub> – that is produced from PGE<sub>2</sub> during infection. We provide  
289 evidence for a possible mechanism for 15-keto PGE<sub>2</sub> via activation of PPAR-  $\gamma$  which is known to promote  
290 anti-inflammatory immune pathways. Finally, we have provided a potential new therapeutic pathway for  
291 treatment of cryptococcal infection as several eicosanoid modulating drugs are approved for patient  
292 treatment (36) .

293 **Materials and methods**

294 (all reagents are from Sigma-Aldrich, UK unless otherwise stated)

295 **Ethics statement**

296 Animal work was performed following UK law: Animal (Scientific Procedures) Act 1986, under  
297 Project License PPL 40/3574. Ethical approval was granted by the University of Sheffield Local  
298 Ethical Review Panel.

299 **Zebrafish**

300 All zebrafish used in this study were the *Nacre* wild type strain. Zebrafish were maintained  
301 according to standard protocols. Adult fish were maintained on a 14:10 – hour light / dark cycle at  
302 28 °C in UK Home Office approved facilities in the Bateson Centre aquaria at the University of  
303 Sheffield.

304 ***C. neoformans***

305 The H99-GFP has been previously described (25). The  $\Delta plb1$ -GFP was generated for this study  
306 by transforming existing deletion mutant strains  $\Delta plb1$  (23) with a GFP expression construct (see  
307 below for transformation protocol). All strains used are in the *C. neoformans* variety *grubii* H99  
308 genetic background.

309 *Cryptococcus* strains were grown for 18 hours at 28 °C, rotating horizontally at 20 rpm.  
310 *Cryptococcus* cultures were pelleted at 3300g for 1 minute, washed twice with PBS (Oxoidm  
311 Basingstoke, UK) and re-suspended in 1ml PBS. Washed cells were then counted with a  
312 haemocytometer and used as described below.

313

314

315 **C. *neoformans* transformation**

316 *C. neoformans* strains  $\Delta plb1$  was biolistically transformed using the pAG32\_GFP transformation  
317 construct as previously described for H99-GFP (25). Stable transformants were identified by  
318 passaging positive GFP fluorescent colonies for at least 3 passages on YPD agar supplemented  
319 with 250  $\mu\text{g/ml}$  Hygromycin B. Two stable  $\Delta plb1$ -GFP transformants were identified (#1-1 and #1-  
320 2), this study uses #1-2 as it was determined to be have the strongest and most homogenous  
321 GFP signal.

322 **J774 Macrophage infection – with exogenous PGE<sub>2</sub> treatment**

323 J774 macrophage infection was performed as previously described (21) with the following  
324 alterations. J774 murine macrophage-like cells were cultured for a minimum of 4 passages in T75  
325 tissue culture flasks at 37°C 5% CO<sub>2</sub> in DMEM (High glucose, Sigma) supplemented with 10%  
326 Fetal Bovine Calf Serum (Invitrogen), 1% 10,000 units Penicillin / 10 mg streptomycin and 1 %  
327 200 mM L – glutamine, fully confluent cells were used for each experiment. Macrophages were  
328 counted by haemocytometer and diluted to a concentration of  $1 \times 10^5$  cells per ml in DMEM  
329 supplemented with 1  $\mu\text{g/ml}$  lipopolysaccharide (LPS from *E. coli*, Sigma L2630) before being  
330 plated into 24 well microplates (Greiner) and incubated for 24 hours (37 °C 5% CO<sub>2</sub>).

331 Following 24-hour incubation, medium was removed and replaced with 1 ml DMEM supplemented  
332 with 2 nM prostaglandin E<sub>2</sub> (CAY14010, 1mg/ml stock in 100% ethanol). Macrophage wells were  
333 then infected with 100  $\mu\text{l}$   $1 \times 10^6$  yeast/ml *Cryptococcus* cells (from overnight culture, washed. See  
334 above) opsonized with anti-capsular IgG monoclonal antibody (18b7, a kind gift from Arturo  
335 Casadevall). Cells were incubated for 2 hours (37 °C 5% CO<sub>2</sub>) and then washed with 37 °C PBS  
336 until extracellular yeast were removed. After washing, infected cells were treated with 1ml DMEM  
337 supplemented with PGE<sub>2</sub>.

338 To calculate IPR, replicate wells for each treatment/strain were counted at 0 and 18 hours. Each  
339 well was washed once with 1ml 37 °C PBS prior to counting to remove any *Cryptococcus* cells  
340 released by macrophage death or vomocytosis. Intramacrophage *Cryptococci* were released by  
341 lysis with 200  $\mu$ l dH<sub>2</sub>O for 20 minutes (lysis confirmed under microscope). Lysate was removed  
342 to a clean microcentrifuge tube and an additional 200  $\mu$ l was used to wash the well to make a  
343 total lysate volume of 400  $\mu$ l. *Cryptococcus* cells within lysates were counted by  
344 haemocytometer. IPR was calculated by dividing the total number of counted yeast at 18hr by the  
345 total at 0hr.

#### 346 **J774 Macrophage co-infection.**

347 J774 cells were prepared and seeded at a concentration of  $1 \times 10^5$  per ml as above in 24 well  
348 microplates and incubated for 24 hours (37 °C 5% CO<sub>2</sub>), 45 minutes prior to infection J774 cells  
349 were activated with 150 ng/ml phorbol 12-myristate 13-acetate in DMSO added to 1 ml serum  
350 free DMEM. Following activation J774 cells were washed and infected with 100  $\mu$ l /  $1 \times 10^6$  yeast/ml  
351 50:50 mix of  $\Delta plb1$  (non-fluorescent) and H99-GFP (e.g.  $5 \times 10^5$   $\Delta plb1$  and  $5 \times 10^5$  H99-GFP).  
352 Infected cells were incubated for 2 hours (37 °C 5% CO<sub>2</sub>) to allow for phagocytosis of  
353 *Cryptococcus* and then washed multiple times with 37 °C PBS to remove unphagocytosed yeast,  
354 each well was observed between washes to ensure that macrophages were not being washed  
355 away. After washing 1 ml DMEM was added to each well.

356 Co-infected cells were imaged over 20 hours using a Nikon TE2000 microscope fitted with a  
357 climate controlled incubation chamber (37 °C 5% CO<sub>2</sub>) using a Digital Sight DS-QiMC camera  
358 and a Plan APO Ph1 20x objective lens (Nikon). GFP and bright field images were captured every  
359 4 minutes for 20 hours. Co-infection movies were scored manually. Co-infected macrophages  
360 that contained 2  $\Delta plb1$  (non-fluorescent) and 1 H99-GFP (GFP positive) yeast cells at 0 hr were  
361 tracked for 18 hours and before the burden of each strain within the macrophage was counted

362 again. The IPR for  $\Delta plb1$  within co-infected macrophages was calculated by dividing the number  
363 of  $\Delta plb1$  cells within a macrophage at 18 hr by the number at 0 hr.

#### 364 **Zebrafish infection**

365 Washed and counted *Cryptococcus* cells were pelleted at 3300g for 1 minute and re-suspended  
366 in 10% Polyvinylpyrrolidone (PVP), 0.5% Phenol Red in PBS to give the required inoculum in 1  
367 nl. This injection fluid was loaded into glass capillaries shaped with a needle puller for  
368 microinjection. Zebrafish larvae were injected at 2-days post fertilisation; the embryos were  
369 anaesthetised by immersion in 0.168 mg/ml tricaine in E3 before being transferred onto microscope  
370 slides coated with 3% methyl cellulose in E3 for injection. Prepared larvae were injected with two  
371 0.5 nl boluses of injection fluid by compressed air into the yolk sac circulation valley. Following  
372 injection, larvae were removed from the glass slide and transferred to E3 to recover from  
373 anaesthetic and then transferred to fresh E3 to remove residual methyl cellulose. Successfully  
374 infected larvae (displaying systemic infection throughout the body and no visible signs of damage  
375 resulting from injection) were sorted using a fluorescent stereomicroscope. Infected larvae were  
376 maintained at 28 °C.

#### 377 **Eicosanoid / receptor agonist treatment of infected zebrafish larvae**

378 All compounds below were purchased from Cayman Chemical. Compounds were resuspended  
379 in DMSO and stored at -20 °C until used. Prostaglandin E<sub>2</sub> (CAY14010, 10mg/ml stock),  
380 Prostaglandin D<sub>2</sub> (CAY12010, 10mg/ml stock), 16,16-dimethyl PGE<sub>2</sub> (CAY14750, 10mg/ml  
381 stock), 15-keto PGE<sub>2</sub> (CAY14720, 10mg/ml stock) and troglitazone (CAY14720, 10mg/ml stock).  
382 Treatment with exogenous compounds during larval infected was performed by adding  
383 compounds (or equivalent solvent) to fish water (E3) to achieve the desired concentration. Fish  
384 were immersed in compound supplemented E3 throughout the experiment from the time of  
385 injection.

## 386 **Zebrafish fungal burden measurement**

387 Individual infected zebrafish embryos were placed into single wells of a 96 well plate (VWR) with  
388 200 ul of E3 (unsupplemented E3, or E3 supplemented with eicosanoids / receptor agonist  
389 depending on the assay). Infected embryos were imaged at 0 days post infection (dpi), 1 dpi, 2  
390 dpi and 3 dpi in their 96 well plates using a Nikon Ti-E with a CFI Plan Achromat UW 2X N.A 0.06  
391 objective lens. Images were captured with a Neo sCMOS (Andor, Belfast, UK) and NIS Elements  
392 (Nikon, Richmond, UK). Images were exported from NIS Elements into Image J FIJI as  
393 monochrome tif files. Images were thresholded in FIJI using the 'moments' threshold preset and  
394 converted to binary images to remove all pixels in the image that did not correspond to the  
395 intensity of the fluorescently tagged *C. neoformans*. The outline of the embryo was traced using  
396 the 'polygon' ROI tool, avoiding autofluorescence from the yolk sac. The total number of pixels in  
397 the thresholded image were counted using the FIJI 'analyse particles' function, the 'total area'  
398 measurement from the 'summary' readout was used for the total number of GFP + pixels in each  
399 embryo.

## 400 **Acknowledgments**

401 We thank the Bateson Centre aquaria staff for their assistance with zebrafish husbandry and the Johnston,  
402 Renshaw and Elks labs for critical discussions. We also thank Arturo Casadevall (Johns Hopkins  
403 University, Maryland USA) for providing the 18b7 antibody.

## 404 **Author Information**

405 The experiments for this study were conceived by RJE, RCM, SAR and SAJ.

406 The experiments for this study were performed by RJE and SN.

407 Analysis was performed by RJE, SN and SAJ.

408 Generation of GFP strains was performed by RJE and EB.

409 The manuscript was written by RJE, RCM, SAR and SAJ. With feedback from EB and SN.

410

411

412

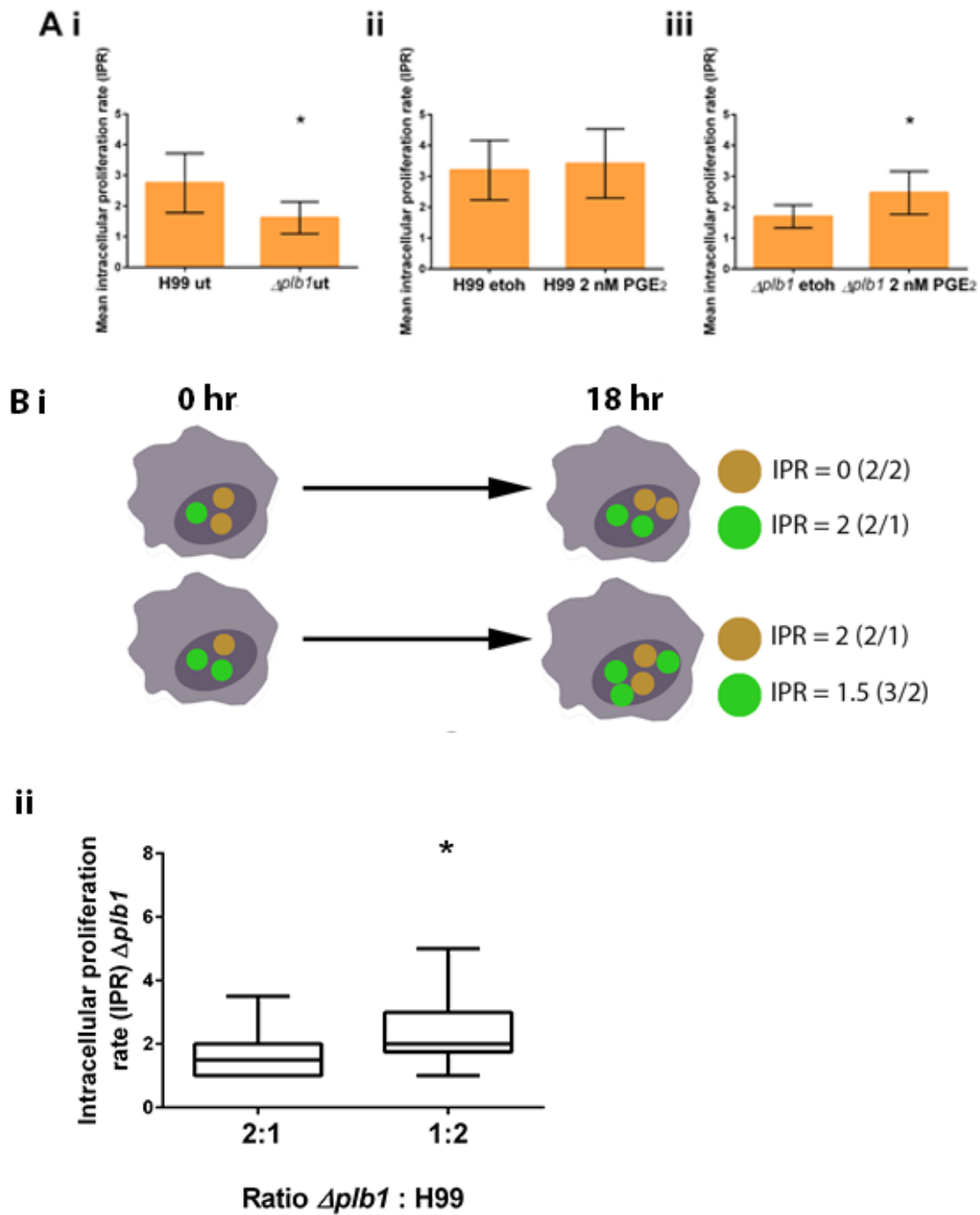
413

414

- 415 (1) Brown GD, Denning DW, Gow NA, Levitz SM, Netea MG, White TC. Hidden killers: human fungal  
416 infections. *Sci Transl Med* 2012 Dec 19;4(165):165rv13.
- 417 (2) Park BJ, Wannemuehler KA, Marston BJ, Govender N, Pappas PG, Chiller TM. Estimation of the  
418 current global burden of cryptococcal meningitis among persons living with HIV/AIDS. *AIDS* 2009  
419 Feb;23:525-530.
- 420 (3) Ma H, May RC. Chapter 5 Virulence in *Cryptococcus* Species. In: Allen I. Laskin, Sima Sariaslani and  
421 Geoffrey M. Gadd, editor. : Academic Press; 2009. p. 131-190.
- 422 (4) Gibson JF, Johnston SA. Immunity to *Cryptococcus neoformans* and *C. gattii* during cryptococcosis.  
423 *Fungal Genet Biol* 2015 May;78:76-86.
- 424 (5) Kawakami K, Kohno S, Kadota J, Tohyama M, Teruya K, Kudeken N, et al. T cell-dependent  
425 activation of macrophages and enhancement of their phagocytic activity in the lungs of mice inoculated  
426 with heat-killed *Cryptococcus neoformans*: involvement of IFN-gamma and its protective effect against  
427 cryptococcal infection. *Microbiol Immunol* 1995;39(2):135-143.
- 428 (6) Voelz K, Lammas DA, May RC. Cytokine signaling regulates the outcome of intracellular macrophage  
429 parasitism by *Cryptococcus neoformans*. *Infect Immun* 2009 Aug;77(8):3450-3457.
- 430 (7) Leopold Wager CM, Hole CR, Wozniak KL, Olszewski MA, Wormley FL, Jr. STAT1 signaling is  
431 essential for protection against *Cryptococcus neoformans* infection in mice. *J Immunol* 2014 Oct  
432 15;193(8):4060-4071.
- 433 (8) Chrétien F, Lortholary O, Kansau I, Neuville S, Gray F, Dromer F. Pathogenesis of cerebral  
434 *Cryptococcus neoformans* infection after fungemia. *J Infect Dis* 2002 Aug;186:522-530.
- 435 (9) Charlier C, Nielsen K, Daou S, Brigitte M, Chretien F, Dromer F. PMC2612285; Evidence of a role for  
436 monocytes in dissemination and brain invasion by *Cryptococcus neoformans*. *Infect Immun* 2009  
437 Jan;77:120-127.
- 438 (10) Norris PC, Reichart D, Dumlao DS, Glass CK, Dennis EA. Specificity of eicosanoid production  
439 depends on the TLR-4-stimulated macrophage phenotype. *J Leukoc Biol* 2011 Sep;90(3):563-574.
- 440 (11) Gupta S, Maurya MR, Stephens DL, Dennis EA, Subramaniam S. An integrated model of eicosanoid  
441 metabolism and signaling based on lipidomics flux analysis. *Biophys J* 2009 Jun 3;96(11):4542-4551.
- 442 (12) Harizi H. The immunobiology of prostanoid receptor signaling in connecting innate and adaptive  
443 immunity. *Biomed Res Int* 2013;2013:683405.
- 444 (13) Angeli V, Faveeuw C, Roye O, Fontaine J, Teissier E, Capron A, et al. Role of the parasite-derived  
445 prostaglandin D2 in the inhibition of epidermal Langerhans cell migration during schistosomiasis infection.  
446 *J Exp Med* 2001 May 21;193(10):1135-1147.
- 447 (14) Ahmadi M, Emery DC, Morgan DJ. Prevention of both direct and cross-priming of antitumor CD8+ T-  
448 cell responses following overproduction of prostaglandin E2 by tumor cells in vivo. *Cancer Res* 2008 Sep  
449 15;68(18):7520-7529.
- 450 (15) Harizi H, Corcuff JB, Gualde N. Arachidonic-acid-derived eicosanoids: roles in biology and  
451 immunopathology. *Trends Mol Med* 2008 Oct;14:461-469.

- 452 (16) Noverr MC, Erb-Downward JR, Huffnagle GB. Production of eicosanoids and other oxylipins by  
453 pathogenic eukaryotic microbes. *Clin Microbiol Rev* 2003 Jul;16(3):517-533.
- 454 (17) Erb-Downward JR, Huffnagle GB. *Cryptococcus neoformans* produces authentic prostaglandin E2  
455 without a cyclooxygenase. *Eukaryot Cell* 2007 Feb;6(2):346-350.
- 456 (18) Erb-Downward JR, Noggle RM, Williamson PR, Huffnagle GB. The role of laccase in prostaglandin  
457 production by *Cryptococcus neoformans*. *Mol Microbiol* 2008 Jun;68(6):1428-1437.
- 458 (19) Noverr MC, Cox GM, Perfect JR, Huffnagle GB. PMC148814; Role of PLB1 in pulmonary  
459 inflammation and cryptococcal eicosanoid production. *Infect Immun* 2003 Mar;71:1538-1547.
- 460 (20) Shen L, Liu Y. Prostaglandin E2 blockade enhances the pulmonary anti-*Cryptococcus neoformans*  
461 immune reaction via the induction of TLR-4. *Int Immunopharmacol* 2015 Sep;28(1):376-381.
- 462 (21) Evans RJ, Li Z, Hughes WS, Djordjevic JT, Nielsen K, May RC. Cryptococcal Phospholipase B1  
463 (Plb1) is required for intracellular proliferation and control of titan cell morphology during macrophage  
464 infection. *Infect Immun* 2015 Jan 20.
- 465 (22) Bojarczuk A, Miller KA, Hotham R, Lewis A, Ogryzko NV, Kamuyango AA, et al. *Cryptococcus*  
466 *neoformans* Intracellular Proliferation and Capsule Size Determines Early Macrophage Control of  
467 Infection. *Sci Rep* 2016 Feb 18;6:21489.
- 468 (23) Cox GM, McDade HC, Chen SC, Tucker SC, Gottfredsson M, Wright LC, et al. Extracellular  
469 phospholipase activity is a virulence factor for *Cryptococcus neoformans*. *Mol Microbiol* 2001 Jan;39:166-  
470 175.
- 471 (24) Voelz K, Johnston SA, Smith LM, Hall RA, Idnurm A, May RC. 'Division of labour' in response to host  
472 oxidative burst drives a fatal *Cryptococcus gattii* outbreak. *Nat Commun* 2014 Oct 17;5:5194.
- 473 (25) Voelz K, Johnston SA, Rutherford JC, May RC. Automated analysis of cryptococcal macrophage  
474 parasitism using GFP-tagged cryptococci. *PLoS One* 2010 Dec 31;5(12):e15968.
- 475 (26) Feng Y, Renshaw S, Martin P. Live imaging of tumor initiation in zebrafish larvae reveals a trophic  
476 role for leukocyte-derived PGE(2). *Curr Biol* 2012 Jul 10;22(13):1253-1259.
- 477 (27) North TE, Goessling W, Walkley CR, Lengerke C, Kopani KR, Lord AM, et al. Prostaglandin E2  
478 regulates vertebrate haematopoietic stem cell homeostasis. *Nature* 2007 Jun 21;447(7147):1007-1011.
- 479 (28) Chayakulkeeree M, Johnston SA, Oei JB, Lev S, Williamson PR, Wilson CF, et al. SEC14 is a  
480 specific requirement for secretion of phospholipase B1 and pathogenicity of *Cryptococcus neoformans*.  
481 *Mol Microbiol* 2011 May;80:1088-1101.
- 482 (29) Ohno H, Morikawa Y, Hirata F. Studies on 15-hydroxyprostaglandin dehydrogenase with various  
483 prostaglandin analogues. *J Biochem* 1978 Dec;84(6):1485-1494.
- 484 (30) Chou WL, Chuang LM, Chou CC, Wang AH, Lawson JA, FitzGerald GA, et al. Identification of a  
485 novel prostaglandin reductase reveals the involvement of prostaglandin E2 catabolism in regulation of  
486 peroxisome proliferator-activated receptor gamma activation. *J Biol Chem* 2007 Jun 22;282(25):18162-  
487 18172.
- 488 (31) Tiefenbach J, Moll PR, Nelson MR, Hu C, Baev L, Kislinger T, et al. A live zebrafish-based screening  
489 system for human nuclear receptor ligand and cofactor discovery. *PLoS One* 2010 Mar 22;5(3):e9797.

- 490 (32) Tenor JL, Oehlers SH, Yang JL, Tobin DM, Perfect JR. Live Imaging of Host-Parasite Interactions in  
491 a Zebrafish Infection Model Reveals Cryptococcal Determinants of Virulence and Central Nervous  
492 System Invasion. *MBio* 2015 Sep 29;6(5):e01425-15.
- 493 (33) Valdez PA, Vithayathil PJ, Janelsins BM, Shaffer AL, Williamson PR, Datta SK. Prostaglandin E2  
494 suppresses antifungal immunity by inhibiting interferon regulatory factor 4 function and interleukin-17  
495 expression in T cells. *Immunity* 2012 Apr 20;36(4):668-679.
- 496 (34) Coggins KG, Latour A, Nguyen MS, Audoly L, Coffman TM, Koller BH. Metabolism of PGE2 by  
497 prostaglandin dehydrogenase is essential for remodeling the ductus arteriosus. *Nat Med* 2002  
498 Feb;8(2):91-92.
- 499 (35) Lemberger T, Desvergne B, Wahli W. Peroxisome proliferator-activated receptors: a nuclear receptor  
500 signaling pathway in lipid physiology. *Annu Rev Cell Dev Biol* 1996;12:335-363.
- 501 (36) Day RO, Graham GG. Non-steroidal anti-inflammatory drugs (NSAIDs). *BMJ* 2013 Jun 11;346:f3195.
- 502
- 503



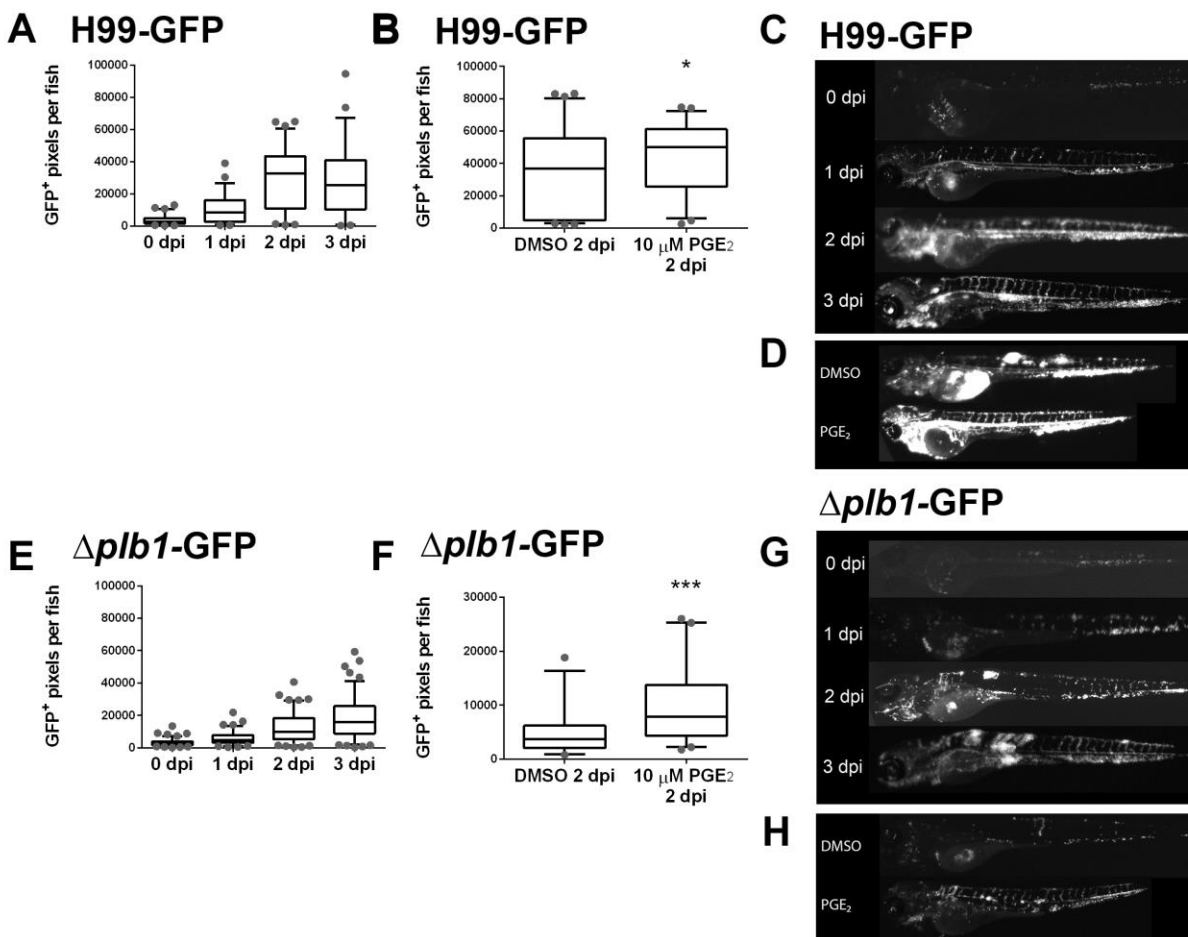
504

505

506 **Fig1**

507 **The intracellular proliferation defect of the *C. neoformans* mutant  $\Delta plb1$ , can be reversed with the**  
508 **addition of exogenous prostaglandin E<sub>2</sub>. A** J774 murine macrophages were infected with  $\Delta plb1$  or the  
509 parental strain H99. Infected cells were left untreated (**i**) or treated with 2 nM PGE<sub>2</sub> (**ii**) or an equivalent  
510 solvent (ethanol) control (**iii**). Mean IPR from 5 biological repeats shown with error bars representing  
511 standard deviation. An unpaired two tailed Student's t-test was performed to compare each treatment  
512 group. (**i**) \* p = 0.0303 (**ii**) ns p = 0.7212 (**iii**) \* p = 0.0376. **B** J774 cells co-infected with a 50:50 mix of  $\Delta plb1$   
513 and H99-GFP. **i** Diagrammatic representation of co-infection experiment. GFP<sup>+</sup> (green) and GFP<sup>-</sup> (yellow)  
514 *C. neoformans* cells within the phagosome were quantified at 0 hr, macrophages with a burden ratio of 1:2  
515 or 2:1 were reanalysed at 18 hr, the IPR for  $\Delta plb1$  within 2:1 and 1:2 co-infected cells was calculated by  
516 dividing the burden at 18hr by burden at 0 hr for GFP<sup>+</sup> (green) or GFP<sup>-</sup> (yellow) cells. **ii** Quantification of  
517 IPR for  $\Delta plb1$  cells within  $\Delta plb1$ :H99-GFP 2:1 or 1:2 co-infected macrophages. At least 38 co-infected  
518 macrophages were analysed for each condition over 4 experimental repeats. Student's T test performed to  
519 compare ratios – 2:1 vs 1:2 \* p = 0.0137.

520



521

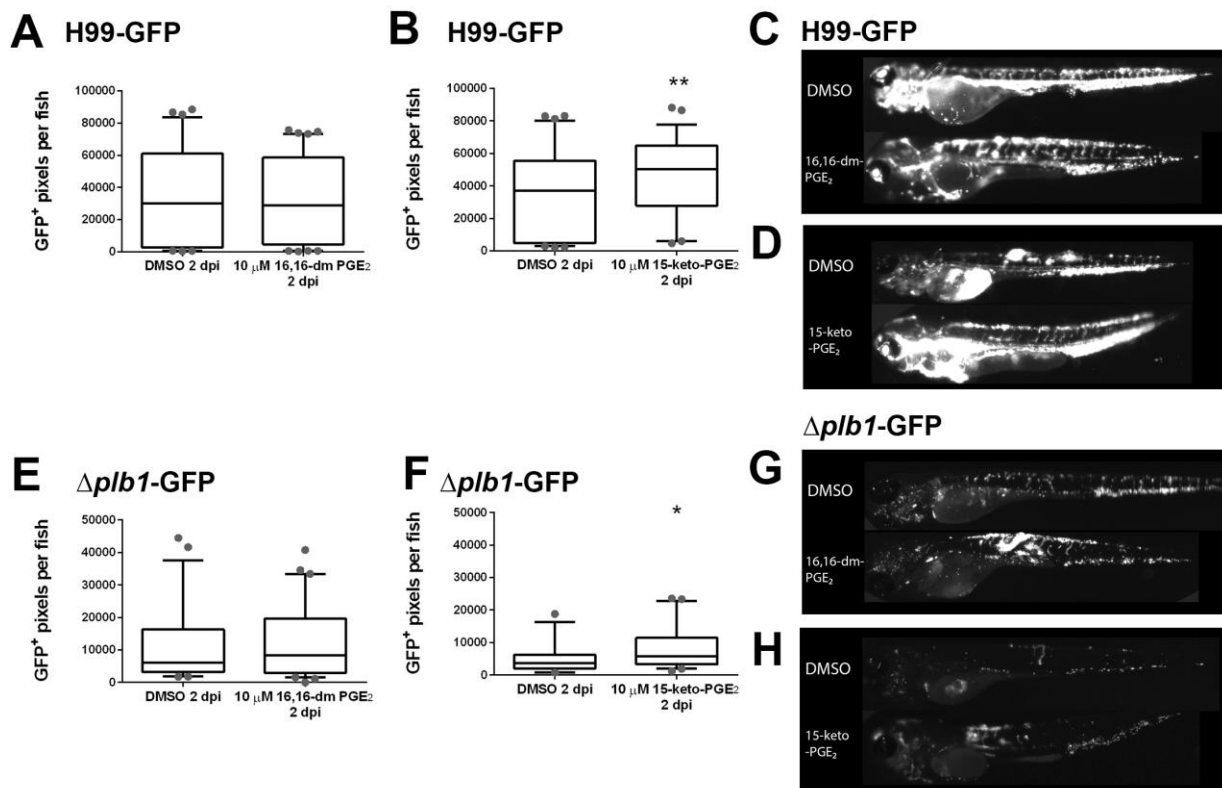
522

523 **Fig2**

524 **The prostaglandin E<sub>2</sub> dependent growth defect of  $\Delta plb1$  is also present *in vivo*: A** H99-GFP infected  
525 larvae imaged at 0, 1, 2 and 3 dpi. At least 50 larvae measured per time point from 3 biological repeats.  
526 Box and whiskers show median, 5<sup>th</sup> percentile and 95<sup>th</sup> percentile. Unpaired Mann-Whitney U tests used to  
527 compare the burden between each strain for every time point, for p values see (Supplementary Fig1). **B** –  
528 H99-GFP Infected larvae treated with 10  $\mu$ M prostaglandin E<sub>2</sub> or equivalent solvent (DMSO) control. At  
529 least 60 larvae measured per treatment group from 3 biological repeats. Box and whiskers show median,  
530 5<sup>th</sup> percentile and 95<sup>th</sup> percentile. Unpaired Mann-Whitney U tests used to compare between treatments  
531 DMSO vs. 10  $\mu$ M PGE<sub>2</sub> \* p = 0.0137 (threshold for significance 0.017, corrected for multiple comparisons).  
532 **C,D** Representative GFP images (representative = median value) of 2dpi H99-GFP infected larvae,  
533 untreated at 0,1,2,3 dpi (**C**) or H99-GFP infected larvae with 10  $\mu$ M PGE<sub>2</sub> at 2dpi (**D**). **E**  $\Delta plb1$ -GFP infected  
534 larvae (500 cell inoculum injected at 2 dpf) imaged at 0, 1, 2 and 3 dpi. N = 3. Box and whiskers show  
535 median, 5<sup>th</sup> percentile and 95<sup>th</sup> percentile. At least 87 larvae measured for each timepoint from 3 biological  
536 repeats. Unpaired Mann-Whitney U tests used to compare the burden between each strain for every time  
537 point, for p values see (Supplementary table 1). **F** –  $\Delta plb1$ -GFP Infected larvae treated with 10  $\mu$ M  
538 prostaglandin E<sub>2</sub> or equivalent solvent (DMSO) control. At least 38 larvae measured per treatment group  
539 from 2 biological repeats. Box and whiskers show median, 5<sup>th</sup> percentile and 95<sup>th</sup> percentile. Unpaired  
540 Mann-Whitney U tests used to compare between treatments  $\Delta plb1$ -GFP DMSO vs 10  $\mu$ M PGE<sub>2</sub> \*\*\* p =  
541 0.0001 (threshold for significance 0.017, corrected for multiple comparisons). **G,H** Representative GFP  
542 images (representative = median value) of 2dpi  $\Delta plb1$ -GFP infected larvae, untreated at 0,1,2,3 dpi (**G**) or  
543  $\Delta plb1$ -GFP infected larvae with 10  $\mu$ M PGE<sub>2</sub> at 2dpi (**H**).

544

545

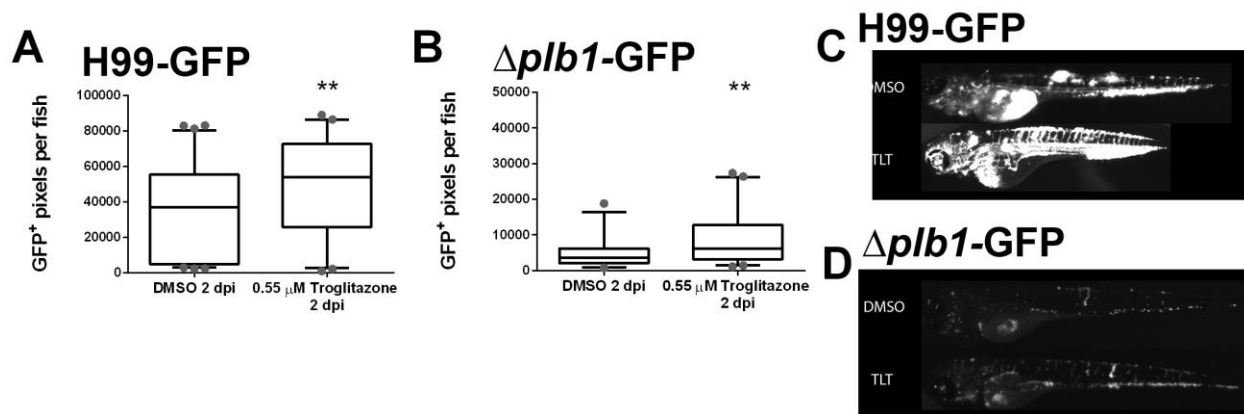


546

547 **Fig3**

548 **The observed activity of PGE<sub>2</sub> is due to its dehydrogenated derivative 15-keto PGE:** Fungal burden  
549 measured at 2 days post infection (2 dpi) by counting GFP positive pixels in each larvae. **A** H99-GFP  
550 Infected larvae treated with 10 μM 16,16-dimethyl prostaglandin E<sub>2</sub> or equivalent solvent (DMSO) control.  
551 At least 75 larvae measured per treatment group from 4 biological repeats. Box and whiskers show median,  
552 5<sup>th</sup> percentile and 95<sup>th</sup> percentile. Unpaired Mann-Whitney U test used to compare between treatments,  
553 DMSO vs. 10 μM 16, 16-dm PGE<sub>2</sub> ns p = 0.9954. **B** H99-GFP Infected larvae treated with 10 μM 15-keto  
554 prostaglandin E<sub>2</sub> or equivalent solvent (DMSO) control. At least 55 larvae measured per treatment group  
555 from 3 biological repeats. Unpaired Mann-Whitney U test used to compare between treatments DMSO vs.  
556 10 μM 15-keto PGE<sub>2</sub> \*\* p = 0.0048 (threshold for significance 0.017, corrected for multiple comparisons).  
557 **C,D** Representative GFP images (representative = median value) of 2dpi H99-GFP infected larvae with 10  
558 μM 16, 16-dimethyl prostaglandin E<sub>2</sub> (**C**) or 10 μM 15-keto prostaglandin E<sub>2</sub> (**D**). **E** *Δplb1-GFP* Infected  
559 larvae treated with 10 μM 16, 16-dimethyl prostaglandin E<sub>2</sub> or equivalent solvent (DMSO) control. At least  
560 45 larvae per treatment group from 3 biological repeats. Unpaired Mann-Whitney U test used to compare  
561 between treatments *Δplb1-GFP* DMSO vs 10 μM 16, 16-dm PGE<sub>2</sub> ns p = 0.9782. **F** *Δplb1-GFP* Infected  
562 larvae treated with 10 μM 15-keto prostaglandin E<sub>2</sub> or equivalent solvent (DMSO) control. At least 38 larvae  
563 measured per treatment group from 2 biological repeats. Unpaired Mann-Whitney U test used to compare  
564 between treatments DMSO vs 10 μM 15-keto PGE<sub>2</sub> \* p = 0.0119 (threshold for significance 0.017, corrected  
565 for multiple comparisons).. **G,H** Representative GFP images (representative = median value) of 2dpi *Δplb1-*  
566 *GFP* infected larvae with 10 μM 16,16-dm PGE<sub>2</sub> (**G**) or 10 μM 15-keto PGE<sub>2</sub> (**H**)

567

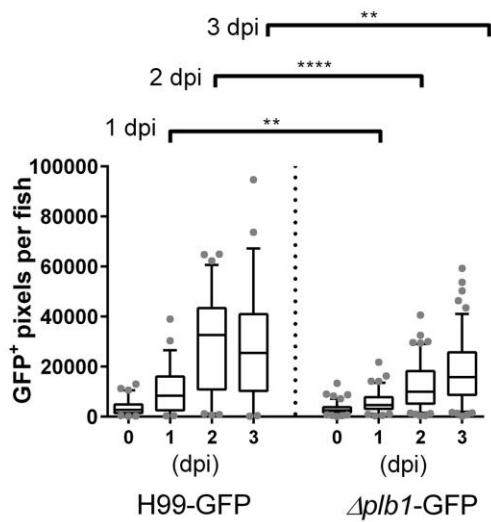


568

569 **Fig4**

570 **15-keto PGE<sub>2</sub> may promote fungal burden by activating host PPAR- $\gamma$ .** 2 day old (2 dpf) *Nacre* zebrafish  
571 larvae injected with 500 cell inoculum. Fungal burden measured at 2 days post infection (2 dpi) by counting  
572 GFP positive pixels within each larvae. **A** H99-GFP Infected larvae treated with 0.55  $\mu$ M Troglitazone (TLT)  
573 equivalent solvent (DMSO) control. Box and whiskers show median, 5<sup>th</sup> percentile and 95<sup>th</sup> percentile. At  
574 least 55 larvae measured per treatment group over 3 biological repeats. Mann-Whitney U test used to  
575 compare between treatments, DMSO vs. 0.55  $\mu$ M Troglitazone \*\* p = 0.0044. **B**  $\Delta$ *plb1-GFP* infected larvae  
576 treated with 0.55  $\mu$ M Troglitazone (TLT) equivalent solvent (DMSO) control. Box and whiskers show  
577 median, 5<sup>th</sup> percentile and 95<sup>th</sup> percentile. At least 39 larvae measured per treatment group from 2 biological  
578 repeats. Mann-Whitney U test used to compare between treatments, DMSO vs. 0.55  $\mu$ M Troglitazone \*\* p  
579 = 0.0089. **C,D** Representative GFP images (representative = median value) of 2dpi H99-GFP infected  
580 larvae with 0.55  $\mu$ M TLT (**C**) or  $\Delta$ *plb1-GFP* infected larvae with 0.55  $\mu$ M TLT (**D**)

**A**



**B**

DPI (H99-GFP vs. $\Delta plb1$ -GFP)	P value
0	ns p = 0.4980
1	** p = 0.0095
2	**** p = <0.0001
3	** p = 0.0013

581

582

583 **Supplementary Fig 1**

584 **Comparison of fungal burden between H99-GFP and  $\Delta plb1$ -GFP infected larvae A** (Data reproduced  
585 from Fig2 A and E for clarity) H99-GFP and  $\Delta plb1$ -GFP infected larvae imaged at 0, 1, 2 and 3 dpi. At  
586 least 50 larvae measured per time point from 3 biological repeats. Box and whiskers show median, 5<sup>th</sup>  
587 percentile and 95<sup>th</sup> percentile. Unpaired Mann-Whitney U tests used to compare the burden between  
588 each strain for every time point. **B** Results of Mann-Whitney U tests comparing burden between

589

590

591

592

593

594

595

596